machines

MDPI

Article

Sports Biomechanics Analysis: Assisting Effectiveness Evaluations for Wearable Compliant Elbow Joint Powered Exoskeleton

Huibin Qin [1], Kai Liu [1], Zefeng Zhang [1], Jie Zheng [1], Zhili Hou [2], Lina Li [2] and Ruiqin Li [1,*]

[1] School of Mechanical Engineering, North University of China, Taiyuan 030051, China; qhbsss@nuc.edu.cn (H.Q.); s202302021@st.nuc.edu.cn (K.L.); s202202012@st.nuc.edu.cn (Z.Z.); sz202402044@st.nuc.edu.cn (J.Z.)

[2] School of Mechanical Engineering, Taiyuan University of Technology, Taiyuan 030024, China; houzhili@tyut.edu.cn (Z.H.); lilina@tyut.edu.cn (L.L.)

* Correspondence: liruiqin@nuc.edu.cn

Abstract: Wearing an exoskeleton, the human body constantly experiences mechanical loading. However, quantifying internal loads within the musculoskeletal system remains challenging, especially during unconstrained dynamic activities such as manual material handling. Currently, exoskeleton systems are commonly integrated with sensor technologies to gather data and assess performances. This is mainly performed to evaluate the physical exoskeletons, and cannot provide real-time feedback during the development phase. Firstly, a powered wearable elbow exoskeleton with variable stiffness is proposed. Through theoretical calculation, the power efficiency formula of exoskeleton is derived. Then, a human musculoskeletal model is built using the AnyBody Modeling System and coupled to the elbow exoskeleton. Under set experimental conditions, the simulation reveals that, when compared with the exoskeleton, the biceps and triceps muscle force parameters of the human model were reduced by 24% and 12%. The muscle activity was diminished by 28–31%, and muscle length shortened by about 6%, in comparison to the condition without the exoskeleton. Finally, through the muscle force experiment, it was verified that the power efficiency of the elbow exoskeleton in the real transport was about 18%. The project reduces costs in the development phase of the exoskeleton and can provide new insights into muscle function and sports biomechanics.

Keywords: powered wearable elbow; compliant variable-stiffness actuators; sports biomechanics; musculoskeletal modeling; assist performance evaluation

check for updates

Academic Editor: Raffaele Di Gregorio

Received: 9 January 2025
Revised: 10 February 2025
Accepted: 18 February 2025
Published: 19 February 2025

Citation: Qin, H.; Liu, K.; Zhang, Z.; Zheng, J.; Hou, Z.; Li, L.; Li, R. Sports Biomechanics Analysis: Assisting Effectiveness Evaluations for Wearable Compliant Elbow Joint Powered Exoskeleton. *Machines* **2025**, *13*, 168. https://doi.org/10.3390/machines13020168

Copyright: © 2025 by the authors. Licensee MDPI, Basel, Switzerland. This article is an open access article distributed under the terms and conditions of the Creative Commons Attribution (CC BY) license (https://creativecommons.org/licenses/by/4.0/).

1. Introduction

Manual material handling (MMH) encompasses activities such as lifting, loading, unloading, pushing, pulling, and holding, which are often repetitive, periodic, and continuous [1]. Carrying for long periods of time increases the risk of muscle damage [2]. Industrial exoskeletons have emerged as a compelling solution to various workplace challenges. They are adept at alleviating physical strain on workers, diminishing fatigue, and enhancing both the comfort and efficiency of the workforce [3]. The MAPS-E upper limb exoskeleton offers intelligent electrical assistance to the shoulders and arms of its users. This equipment can provide workers with 50% of the help effect, thereby reducing employee turnover and providing robust assurance of enhanced production efficiency [4]. With a global vision, Maibao Intelligent Technology is committed to technological research and development and achieving the transformation of wearable powered exoskeletons, which are mainly

applied in industrial logistics, construction, and other industries [5]. Assisted exoskeletons developed abroad include BLEEX, developed by Berkeley University in the United States [6], and HAL, developed by the team of the University of Tsukuba in Japan [7], among others.

However, human bodies with exoskeletons constantly undergo dynamic mechanical loading during movement and locomotion. Excessive loading within the body can lead to fatigue and increase the risk of injury [8]. With the rapid advancement and widespread adoption of exoskeleton robotics, it is essential to quantify the internal mechanical load within the musculoskeletal system and translate physiological changes into performance metrics for exoskeletons. Evaluating the functionality, safety, and feasibility of these devices is critical for risk assessment and injury prevention in movement and ergonomics [9]. This method will also serve to guide research and development efforts, product refinement, and clinical applications of exoskeleton technology [10]. Currently, the majority of evaluation metrics for exoskeletons are relatively simplistic, potentially leading to incomplete assessment outcomes owing to a narrow scope of focus. Farris et al. [11] pointed out that the total metabolic energy consumption of the ankle muscles was not significantly reduced, despite the substantial reduction in plantar flexor muscle strength during the use of elastic ankle exoskeletons. Carlson et al. [12] established an evaluation standard system for military exoskeletons, but this evaluation system only targeted military exoskeletons without considering environmental factors. A large number of studies proved that it is feasible to conduct the real-time feedback control of exoskeleton combined with advanced sensor systems. Zheng Guo Li's team at the National University of Singapore Suzhou Research Institute developed an exoskeleton sensing system based on friction nanogenerators. The system realizes the real-time monitoring of linear displacement, rotation, torsion, bending, and other movements through bidirectional quantitative monitoring. The sensor has the advantages of a simple structure, a low cost, and low power consumption and is suitable for various human–computer interaction scenarios. The HAL exoskeleton system at the University of Tsukuba in Japan uses devices such as angle sensors, EMG sensors, and ground contact force sensors to obtain information about the wearer's state. The HAL system enables automatic control and comfortable power-assisted control based on biofeedback through a hybrid control system, which can adjust the action of the exoskeleton in real time according to the wearer's motion intention.

In this research, the aim is to design a powered compliant elbow joint exoskeleton and evaluate the performance of the exoskeleton as comprehensively as possible by quantifying the power-assisted performance through a method of establishing musculoskeletal model. To achieve this goal, this research uses the AnyBody Modeling System to simulate a musculoskeletal model with an exoskeleton. Through the inverse dynamics analysis of the integrated human–machine model, the relevant parameters of the arm muscles were simulated. Finally, we experimentally demonstrated the feasibility of using the AnyBody simulation to quantify and estimate the exoskeleton-assisted performance in a range of unconstrained real-world tasks, including lifting and walking.

2. Mechanical Structure Design of Powered Compliant Elbow Joint Exoskeleton

The main issue in designing powered compliant elbow joint exoskeletons lies in analyzing the characteristics of the manual material handling movement. Subsequently, it is essential to conduct the safe and normative design of the structure to guarantee that the exoskeleton has excellent compatibility with the human body, thereby achieving a better power effect.

2.1. Physiological Parameters of Human Elbow Joint

According to the description of human physiological structure in anatomy, the standing posture of the human body is defined as the transverse plane, frontal plane, and sagittal plane [13]. The elbow joint is the main joint used to complete the carrying movement, and it can achieve flexion, extension, and rotation [14]. Because the elbow joint does not fully conform to the ideal ball-and-socket joint, the axis of motion changes during actual movement. Therefore, the motion characteristics of the elbow joint on the sagittal plane will be discussed.

Elbow flexion, extension movements, and muscle distribution are shown in Figure 1. Each joint and muscle plays a unique role in its assigned position, working together to maintain the stability and compliance of the elbow joint [15].

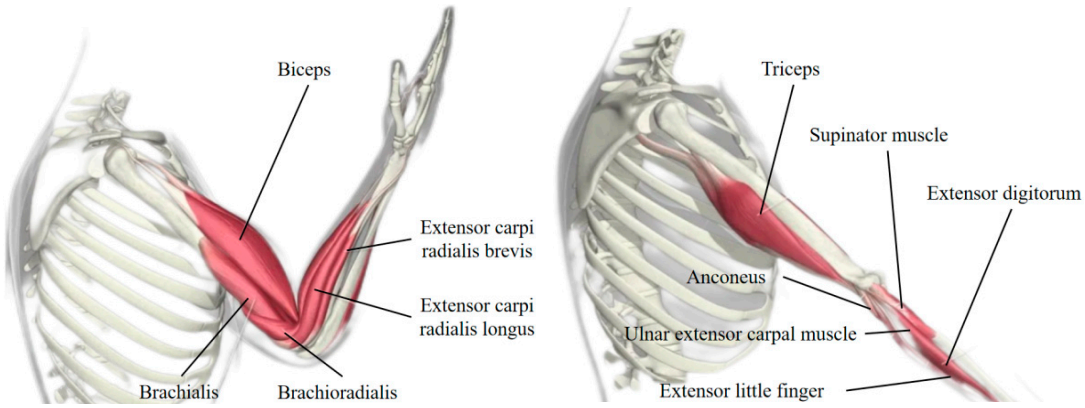


Figure 1. Muscle stress of elbow flexion and extension [16]. (**a**) Elbow flexion. (**b**) Elbow extension.

The elbow joint stress fluctuates in accordance with the nature of the exercise performed. As a key weight-bearing joint, the elbow endures the maximum joint force when it is in a fully extended position. Due to its physiological structure, the elbow joint cannot be overextended or bent backwards [17]. The motion characteristics of the human elbow joint are concisely summarized in Table 1.

Table 1. Movement characteristics of the elbow joint.

Upper Limb Exercise	Argument
Maximum range of elbow flexion and extension angles	(0–135°), 0°
Maximum internal rotation angle of elbow joint	80°
Maximum external rotation angle of elbow joint	85°
Flex 90° muscle tone	8–22 kg
Range of normal motion stiffness of human joint	3–14 N m/rad
Muscle tension during eating activities	30 kg
Maximum peak position of joint motion muscle tension	170 kg

2.2. Mechanical Structure Design of Elbow Exoskeleton

To achieve the best performance, the structural design of the elbow joint-assisted exoskeleton should adhere to the principles of bionics, the principles of safety and reliability, as well as those of human–machine interaction.

In order to ensure the power efficiency of the elbow exoskeleton, the structure design needs to consider the size of the elbow joint, the material selected by the main body, the material of the elastic element, and the matching method. Figure 2 shows the integrated

design of the powered wearable compliant elbow joint exoskeleton. It is mainly composed of an upper arm plate, a lower arm plate, a binding device, and an elbow sleeve.

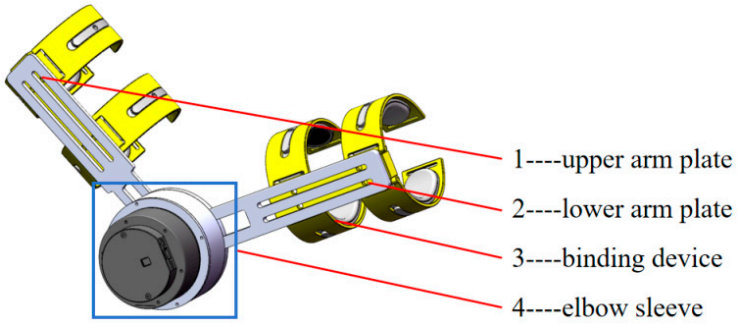


Figure 2. Powered wearable compliant elbow joint exoskeleton structure design schematic diagram.

The internal structure of the powered wearable compliant elbow joint exoskeleton is shown in Figure 3. The upper arm plate is fixed with the exoskeleton shell, and the lower arm plate is connected to the output flange. The wearer fixes the upper and lower arm plates on the forearm and the upper arm using the binding device. The input flange is used as the input end and the external driving servo motor is connected. The flexible unit is a combination of elastic elements and pulleys. The torque transmitted from the input flange passes through the elastomer and produces attenuation, so that it cannot be completely transmitted to the output flange. The two produce relative rotation, so that the whole mechanism has the characteristics of flexible drive.

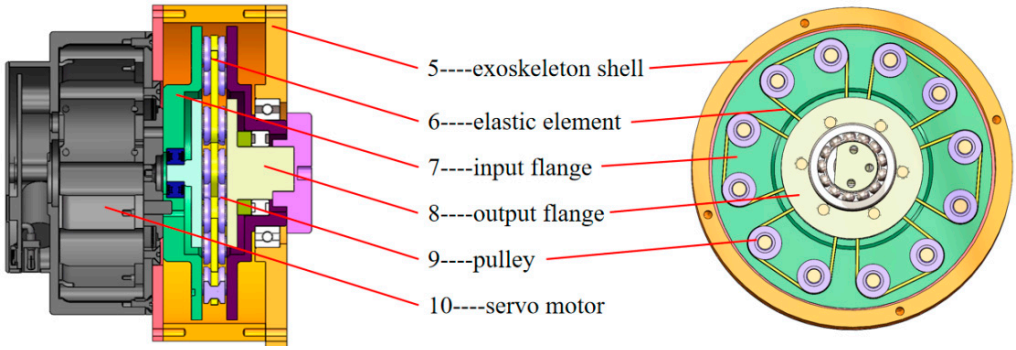


Figure 3. Internal structure design of the variable stiffness compliant elbow joint.

Based on the parametric research of the human elbow joint, the geometric parameters of the variable-stiffness compliant drive mechanism are shown in Table 2. The designed parameters conform to the characteristics of miniaturization and can withstand large tension without failure.

Table 2. Geometrical parameters of the variable-stiffness compliant actuator.

Argument	Instructions	Numerical Value
N	Number of branches of flexible unit	1–6
d	PU circular belt diameter	2 mm
ρ	PU circular belt density	1.0×10^{-6} kg/mm^3
E	Modulus of elasticity	50.955 N/mm^2
L_1	Length of component 1	15 mm
L_2	Length of component 2	34 mm
F_o	Preload	5 N
k	Stiffness of elastic element	0.735 N m/rad

The wearable powered elbow exoskeleton is driven by a motor, and the output torque is transmitted to the variable-stiffness flexible drive module. Due to the role of the internal flexible unit of the flexible drive module, the torque is attenuated and then transmitted to the lower arm, which drives the rotation of the lower arm relative to the upper arm and realizes the flexion and extension of the elbow joint. This ensures that the exoskeleton has good compatibility with the human body to obtain a better dynamic effect.

The stiffness k of the elastic element plays a key role in determining the performance of the designed variable-stiffness compliant drive mechanism. The servo motor is directly connected to the housing of the elbow sleeve, with the advantage that the transmission between the two can be omitted, reducing energy loss and greatly reducing the volume of the powered compliant elbow joint. The lightweight structural designs places little load on the human body. It can provide greater force assistance, reduce energy loss in the process of power transmission, and improve overall work efficiency.

The elbow exoskeleton is actuated through the MG6012Ev2 (manufactured by Hillhouse Control Technology Co., LTD., Shanghai, China) brushless DC servo motor, featuring an integrated electric drive design that includes a built-in FOC (Field-Oriented Control) driver and an 18-bit absolute encoder. Communication with the motor is achieved via the CAN protocol. The motor peak output torque of 16 N m satisfies the operational requirements. Table 3 summarizes the motor parameters.

Table 3. MG6012Ev2 motor parameters.

Item	Argument
Rated voltage	48 V
Rated torque	6 N m
Rated speed	256 rpm
Rated current	3.5 A
Peak power	294 w
Peak torque	16 N m

The servo motor is equipped with an adaptive reducer model PG4108, which has a reduction ratio of 8. The rated static load capacity of the bearing is 906 N, and the total weight of a single elbow joint is 1.108 kg. Exoskeletons need to match the arm lengths of different human bodies and account for ergonomics as well as wearer comfort requirements. This design refers to the Chinese adult body size standard GB/T10000-2023, and the arm plate is designed as an adjustable mechanism [18]. The upper arm plate adjustment range is 250–360 mm, the adjustment range of the forearm plate is 185–280 mm.

In the field of artificial material handling, powered wearable exoskeletons are receiving more and more attention [19]. A radial adjustable stiffness structure design increases the flexibility between the elbow exoskeleton and the human body while also improving safety and providing greater assistance to the porter.

3. Dynamic Analysis of the Powered Wearable Compliant Elbow Joint Exoskeleton

The objective of conducting dynamic analyses for an elbow joint-assisted exoskeleton is to ensure the robotic system can perform the designated motion tasks with precision and efficiency. This is crucial for achieving the desired level of assistance in manual tasks and lays the groundwork for the development of a compliant drive system and control system within the robot design framework [20].

3.1. Theoretical Analysis of Dynamics

The essence of dynamic analysis lies in establishing equations that describe the relationship between force–mass–acceleration and torque–inertia–angular acceleration [21]. This process is essential for calculating the forces or torques acting on the object, which in turn provides the necessary foundation for selecting an appropriate driving source and devising a control strategy for the robot [22].

Dynamic analysis typically employs two principal approaches, i.e., Newtonian mechanics and Lagrange mechanics. The Newtonian mechanics method is particularly well suited for systems characterized by a straightforward structure and low degrees of freedom [23].

The Newton–Euler method represents the inaugural approach to dynamic modeling and analysis. The Newtonian equations elucidate the interplay between external forces, mass, and the acceleration of the center of mass in a translating rigid body [24]. Concurrently, Euler equations delineate the relationship between external torques, angular acceleration, angular velocity, and the inertia tensor in a rotating rigid body. Consequently, the Newton–Euler equations are capable of encapsulating the dynamics of a rigid body by describing the nexus of forces, inertia, and acceleration, thereby facilitating the formulation of the dynamic equations governing the rigid body motion [25].

3.2. Dynamic Analysis of the Wearable Elbow Joint Powered Exoskeleton

Sports biomechanics is an interdisciplinary field that applies the fundamental principles of statics, kinematics, and dynamics, alongside anatomical and physiological knowledge, to perform quantitative analyses of human motion [26]. To streamline the computation of torque at the elbow joint within a static framework, the handling model is simplified, as illustrated in Figure 4. The model assumes that the subject lifts the box at a controlled, slower pace, thereby mitigating the impact of inertial forces on the human body. It ensures that the force conditions in both arms are nearly identical, thereby simplifying the subsequent analysis of torque at the elbow joint.

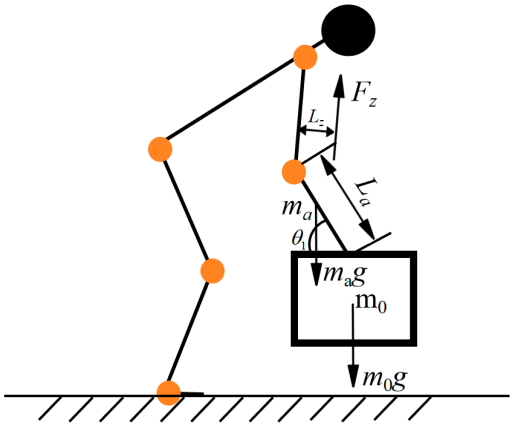


Figure 4. Simplified mechanical model of human body handling.

L_a and L_z denote the distances from the elbow to the wrist, specifically the length of the forearm and the length of the moment arm produced by the elbow flexor. θ_1 represents the angle between the forearm and the upper plane of the box. m_0 and m_a denote the mass of the lifted object and the mass of the forearm, respectively. F_z represents the force generated by the elbow flexor when lifting the box.

The torque M_0 generated via the weight on the elbow joint is derived as shown in Equation (1):

$$M_0 = m_0 g \cos\theta_1 L_a \quad (1)$$

The forearm torque on the elbow joint M_a is given in Equation (2):

$$M_a = 1/2 m_a g \cos\theta_1 L_a \tag{2}$$

Torque M_z generated via the elbow flexor on the elbow joint can be calculated using Equation (3):

$$M_z = F_z L_z \tag{3}$$

According to the principle of torque balance, the torque generated through the arm muscles when the elbow exoskeleton is not worn, M_z, is expressed as shown in Equation (4):

$$M_z = M_0 + M_a \tag{4}$$

M_z can be obtained as shown in Equation (5):

$$M_z = m_0 g \cos\theta_1 L_a + 1/2 m_a g \cos\theta_1 L_a \tag{5}$$

The force of elbow flexor muscle F_z can be obtained as follows:

$$F_z = g \cos\theta_1 L_a \frac{m_0 + 1/2 m_a}{L_z} \tag{6}$$

According to Equation (6), it is evident that when lifting heavy objects, the force exerted by the elbow flexor is primarily associated with the mass of the object and the angle between the forearm and the horizontal plane during the lifting process. It can be observed that the greater the value of m_0 and the smaller the value of θ_1, the greater the force required from the elbow flexor.

From the standpoint of elbow joint-assisted exoskeleton design, the act of lifting heavy objects primarily neutralizes the downward gravitational force through the engagement of muscles, including the biceps and deltoids. The power model depicted in Figure 5 illustrates the configuration after the subject dons the elbow joint-assisted exoskeleton.

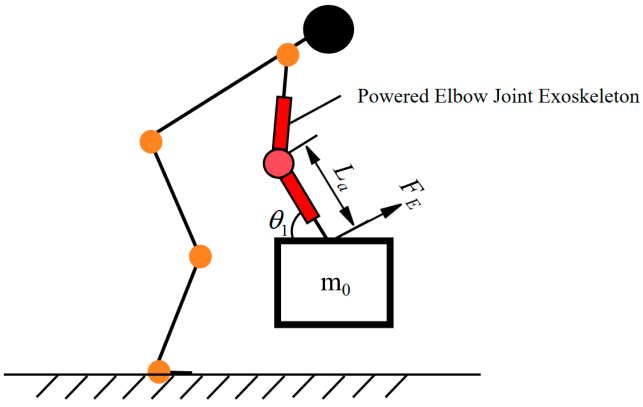


Figure 5. Simplified mechanical model of human carrying action after wearing elbow joint.

An elbow exoskeleton creates a torque on the elbow joint of the arm, M_E. This is derived as shown in Equation (7):

$$M_E = F_E L_a \tag{7}$$

At this juncture, the torque $M_{Z'}$ generated via the flexor muscles of the elbow joint ensures a torque balance, thus maintaining stability during the lifting movement:

$$M_E + M_{Z'} = M_0 + M_a \tag{8}$$

$M_{Z'}$ can be obtained as shown in Equation (9):

$$M_{Z'} = m_0 g \cos\theta_1 L_a + 1/2 m_a g \cos\theta_1 L_a - F_E L_a \tag{9}$$

The strength $F_{Z'}$ of the elbow flexor muscle is enhanced after wearing the elbow joint exoskeleton:

$$F_{z'} = \frac{g \cos\theta_1 L_a (m_0 + 1/2 m_a) - F_E L_a}{L_z} \tag{10}$$

The efficiency η of the elbow exoskeleton in assisting the flexor muscle can be determined as follows:

$$\eta = \frac{F_z - F_{z'}}{F_z} \times 100\% = \frac{F_E}{g \cos\theta_1 (m_0 + 1/2 m_a)} \tag{11}$$

In typical handling scenarios, the θ_1 range of motion typically spans from 0° to 90°. As a result, the assist efficiency, η, exhibits a positive correlation with the rise in θ_1 and F_E, whereas it diminishes as m_0 increases. The increased power efficiency of the elbow exoskeleton markedly augments its capacity to alleviate the wearer load, amplify the strength delivered, and curtail energy expenditure. This efficiency is particularly critical in work environments that require sustained heavy-duty labor or the manipulation of substantial loads, as it optimizes the efficacy of the power assistance provided.

Assuming the exoskeleton maintains maximum power, F_E = 50 N and m_a = 2.5 kg for the forearm. Under normal lifting conditions, assuming the value of θ_1 is 30° and the m_0 is 25 kg, it is necessary to take the gravitational acceleration g = 9.8 m/s^2 and analyze the relationship between the mass of the m_0 and the η. Finally, the researchers must substitute them into Equation (11) to obtain η = 22.52%. Given the challenges experimental subjects face in adhering to the experimental hypothesis, a discrepancy may arise between the experimental outcomes and the theoretical expectations. Therefore, the efficacy of the assistance will be further validated through subsequent simulations and experiments.

4. Modeling and Dynamic Simulation Analysis of Human–Machine System Based on the AnyBody Modeling System

The AnyBody Modeling System is a sophisticated software platform used for musculoskeletal modeling and simulation. It was specifically designed for biomechanics analysis. It enables the creation of comprehensive musculoskeletal models of the human body and the simulation of internal loads, including muscle activity, muscle strength, and joint reactions [27]. This tool is primarily utilized to analyze the dynamics of the human body and the interactions between the human body and its environment, particularly in the context of human–computer interfaces [28].

4.1. Evaluation of AnyBody Exoskeleton Assisting Effectiveness

Evaluation methods for assessing the effectiveness of exoskeleton assistance primarily encompass metabolic cost assessment, bio-electricity signal analysis, kinematic and dynamic parameter evaluation, and work condition performance assessment, among others. Notably, AnyBody7.1.2 stands out as the sole software integrating both ergonomic and biomechanics principles, enabling the comprehensive evaluation of exoskeleton assistance through the importation of a full-scale human musculoskeletal model.

The AnyBody Modeling System process primarily utilizes two fundamental principles: the mechanical model and the muscle model. In this research, the focus is on the application of the muscle model.

In the analysis of the human model, the stress imposed on the muscles is initially taken into account. Generally, the factors influencing muscle stress include muscle length,

the rate of contraction, and the magnitude of the external load applied [29]. As illustrated in Figure 6, this research utilizes the Hill muscle model, which is adept at capturing the interplay between muscle tension, contraction dynamics, and extension. Subsequently, the model underwent further refinement to incorporate additional significant characteristics that arise from muscle power. The Hill model consists of an active contractile element (CE), which simulates the generation of active muscle force; a passive elastic element (PE), representing passive muscle tension; and a tendon elastic component (T).

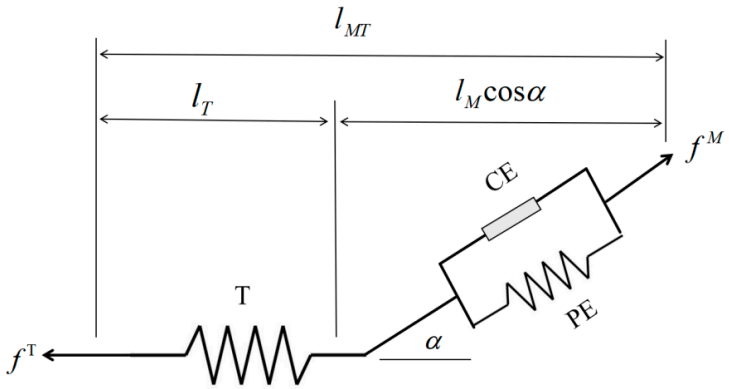


Figure 6. A schematic diagram of the Hill model.

The Hill model offers precise evaluations of muscle force by integrating the significant impact of tendon elasticity on the dynamics of muscle fiber behavior. Furthermore, the synergistic interaction between muscle and tendon is a core element of the model, and is essential for understanding the biomechanics principles it represents.

The length of muscles (l_M), tendons (l_T), and muscle–tendon actuators (l_{MT}) are related as follows in Equation (12)

$$l_{MT} = l_M \cos(\alpha) + l_T \tag{12}$$

4.2. The Construction of Human Body Model and the Analysis of Sports Biomechanics

To accurately simulate real-world handling actions and more effectively assess power efficiency, it is essential to streamline the process of configuring the human body model's parameters. Initially, a new model of the human standing posture must be established within the AnyBody Managed Model Repository (AMMR). Prior to initiating the simulation, the model stature was meticulously set to 178 cm, and its mass was precisely set to 75 kg to ensure that the subject body's parameters were in accordance with the actual situation. We set the coefficient of friction between the palm and the box to 0.8. Given that the human body models within the AnyBody model library are constructed based on the European population standard, it is essential to perform a scaling adjustment on the model prior to simulation.

The percentage governs all human dimensions in accordance with the Gaussian distribution, and the height and weight of the mannequin can be edited in accordance with the statement rules. This adjustment ensures more accurate alignment with the musculoskeletal parameters specific to the subject in question. Implementing these measures is crucial for attaining a high degree of realism and fidelity in the simulation process. The groundwork has been laid for conducting kinematic and dynamics analyses of the model in subsequent stages.

Following the creation of the human musculoskeletal model, the development of an environmental and human interaction model becomes an essential subsequent step. We integrated the box model into the human musculoskeletal model framework, assigning it a mass of 25 kg.

We simulated the behavior of the human body carrying in the AnyBody Modeling System, defined the interactions and constraints between the box and the hand, and ensured a true representation of the physical dynamics involved. We stablished the definitions of the pertinent nodes to ensure seamless synchronization of the box movement with that of the arm, reflecting accurate dynamic interactions within the simulation. A simulation of the processing action is shown in Figure 7.

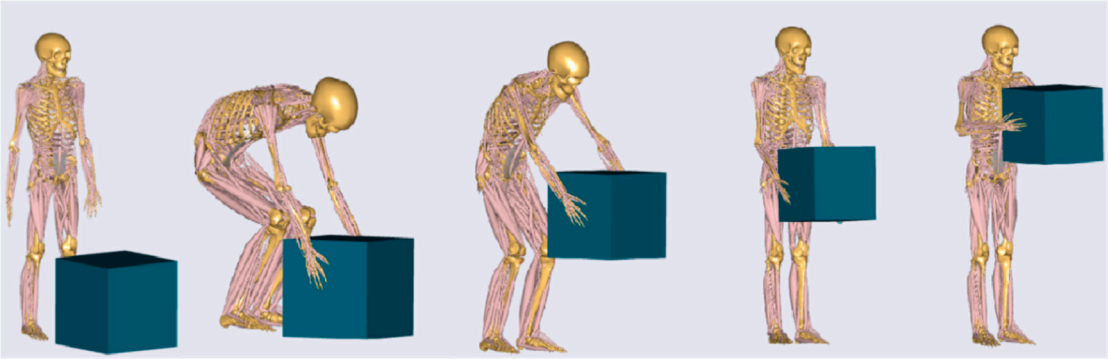


Figure 7. Simulation diagram of handling action.

Within the AnyBody Modeling System, the human body model is capable of executing smooth carrying motions in accordance with the specified commands. The visual representation indicates that the spatial trajectory of the upper limb movement during the model handling process closely aligns with that of actual human handling, thereby validating the accuracy of the established human–box concurrent model.

4.3. Human–Machine Integration Model Establishment

Employing the AnyBody Modeling System, a human–machine model was constructed to simulate and quantify the biomechanics loads experienced by the elbow exoskeleton during transportation tasks. This was performed under conditions both with and without the exoskeleton.

The 3D model of the elbow exoskeleton was established and exported as an ASCII *. STL format file in SolidWorks2023. In order to improve the calculation speed and accuracy, the model should be simplified as much as possible, keeping the upper arm plate, lower arm plate, shaft sleeve, and flexible drive mechanism, eliminating the adjustable part of the environmental model, facilitating the establishment of constraint relations, and removing errors caused by noncritical factors.

The AnyBody Modeling System does not support the simulation of non-rigid bodies. The three connection points of the arm ring are located on the humerus and related muscles of the human model, and node definition is added. Subsequently, the rotation constraint is applied to the *Y*-axis of the elbow joint model, while the constraint on the *Z*-axis is designated as a soft constraint, which allows for more flexible simulation of the joint motion. Ultimately, the joint between the upper and lower arm plates of the mannequin arm and the elbow joint was configured to allow for rotation around the longitudinal axis of the humerus, ensuring an accurate biomechanics representation of joint movement.

As illustrated in Figure 8, the integrated restraint significantly improves the accuracy of the exoskeleton motion tracking, ensuring that it remains stable and is not affected by the torso's swinging motion.

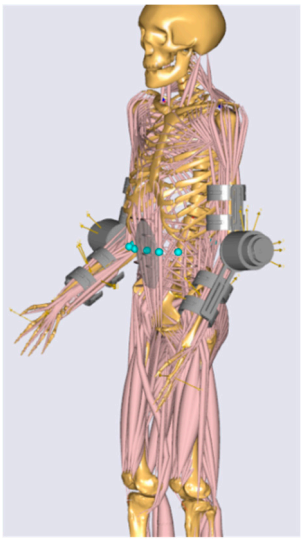


Figure 8. Human–machine integration model in the AnyBody Modeling System.

4.4. Muscle Parameter Analysis

The biceps and triceps were designated as the subjects of the experiment, aiming to analyze variations in muscle strength, activation levels, and length within the human model during the task of carrying a 25 kg box, both prior to and subsequent to donning the powered elbow joint exoskeleton that provides a 50 N boost.

4.4.1. Muscle Force

Muscle force denotes the capacity of the human body, or a particular segment thereof, to overcome internal and external resistance during muscle contractions or extensions. In industrial production environments, workers frequently engage in sustained and repetitive muscle movements, which can lead to muscle fatigue and a consequent diminution in muscular strength [30].

Figure 9 illustrates the comparative force curves of the biceps and triceps muscles, demonstrating the alterations in muscle force dynamics before and after the activation of a wearable compliant powered elbow joint exoskeleton.

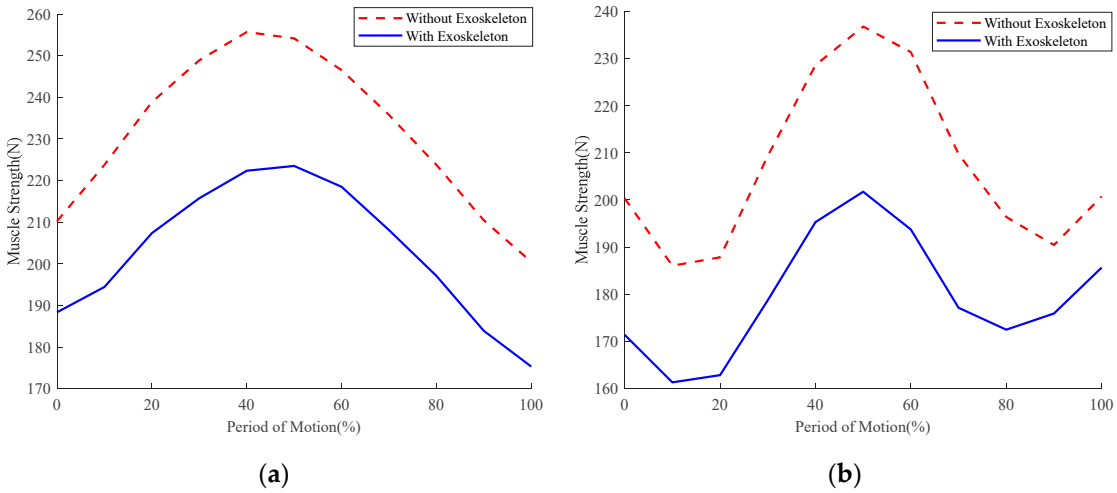


Figure 9. Curve of selected muscle force change. (**a**) Biceps muscle strength change curve. (**b**) Triceps muscle strength change curve.

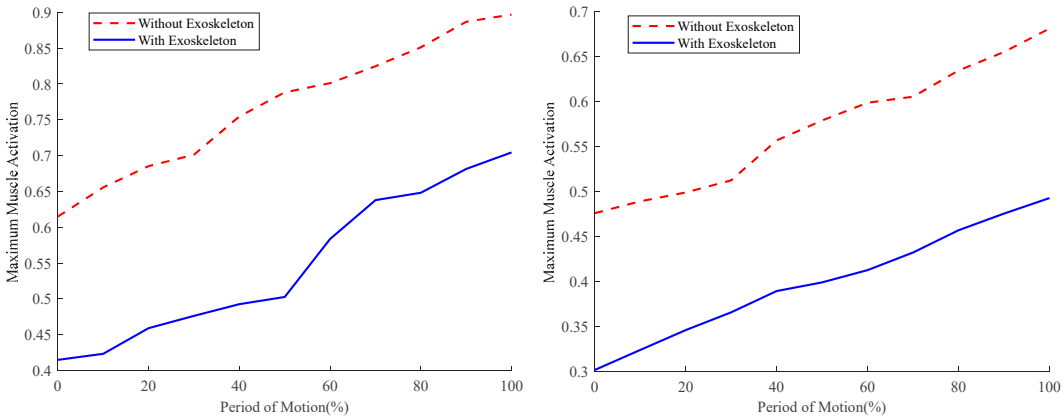
As illustrated in Figure 9a, the application of the powered elbow joint exoskeleton resulted in a reduction of approximately 40 N in the force exerted by the biceps muscle.

The assisting efficiency of the exoskeleton is about 24%. Similarly, as depicted in Figure 9b, the triceps muscle force cancels out by about 30 N following the use of the elbow joint power exoskeleton, and the efficiency is about 12%. It can be concluded that the powered wearable elbow exoskeleton supplies a significant compensatory force to the arm muscles, thereby diminishing the muscular effort that must be exerted by the individual.

4.4.2. Maximum Muscle Activation

The degree of muscle activation denotes the ratio of the force produced from specific muscles or muscle groups to their maximum capacity during human movement, reflecting the extent to which the muscles are engaged. The principle of muscle activation is based on the measurement of muscle electrical signals, performed by measuring the amplitude and frequency of muscle electrical signals to assess the degree of muscle activation [31].

Figure 10a shows the curve of muscle activation of the biceps before and after wearing the elbow exoskeleton. Figure 10b shows the curve of muscle activation of the anterior and posterior triceps muscles while wearing the elbow exoskeleton.



(**a**) (**b**)

Figure 10. Curve of maximum muscle activation. (**a**) Maximum biceps muscle activation. (**b**) Maximum triceps muscle activation.

The experimental results demonstrate that the peak activity levels of both the biceps and triceps muscles remain under the threshold of 100%, both before and after the application of the elbow exoskeleton. This indicates that the muscles are normally active. Significantly, there is a discernible decrease in the maximum muscle activation at each peak after the use of the elbow exoskeleton. The muscle activity in the biceps is reduced by 28%, and the triceps muscle activity decreases by 31%. This suggests that the elbow exoskeleton support device is effective in diminishing muscle exertion, thereby potentially reducing the likelihood of muscle strain injuries.

4.4.3. Muscle Length

The length–tension relationship of a muscle indicates that when a muscle is activated, its length experiences a non-linear response related to muscle tension [32]. Muscular force output diminishes when muscles operate at lengths that are either excessively long or short. Figure 11a shows the curve of biceps muscle length before and after wearing the elbow exoskeleton. Figure 11b shows the curve of triceps muscle length before and after wearing the elbow exoskeleton.

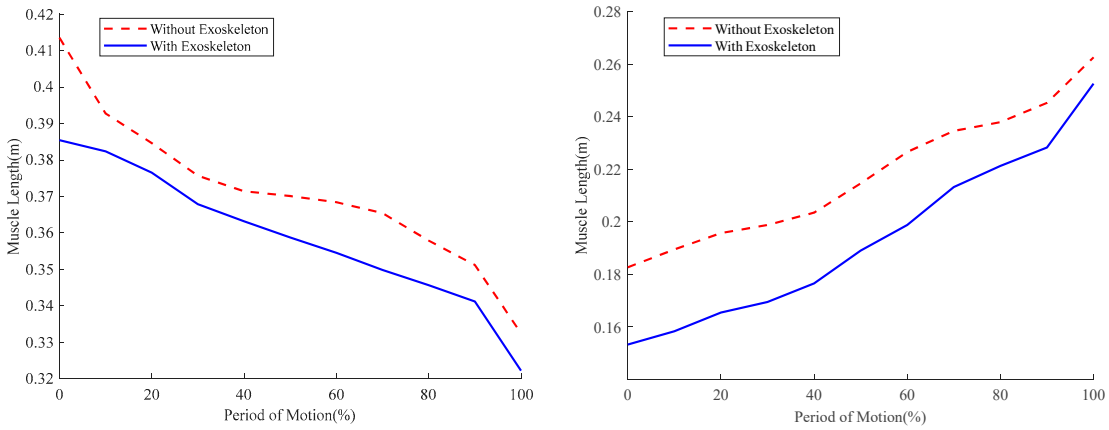


Figure 11. Curve of selected muscle length. (**a**) Bicep length curve. (**b**) Triceps length curve.

The peak muscle length of the biceps following the wearing of the exoskeleton decreased by approximately 3 mm, and that of the triceps was reduced by around 2.5 mm, in contrast to the situation without the exoskeleton being worn. Compared to the muscle length at the moment of relaxation, it is about 6% shorter.

This observation indicates that the elbow joint exerts a compensatory influence on the biceps and triceps muscles, modulating their lengths and potentially optimizing muscle performance.

5. Experimental Investigation on the Wearable Compliant Elbow Joint Powered Exoskeleton

Lift handling experiments were designed to evaluate the power provided by a powered wearable compliant elbow joint exoskeleton. Meanwhile, it also can verify the accuracy of the AnyBody simulation results. Subjects with a height of 178 cm and a weight of 75 kg were selected to wear the elbow dynamic exoskeleton in a safe experimental environment. The power experimental platform and necessary equipment are depicted in Figure 12.



Figure 12. Experimental platform and composition of handling aid.

A sensor band from BioX ApS, Denmark, was adopted to detect human muscle contractions when generating limb motion. This sensor band was integrated with an array of 8 Force Sensitive Resistors (FSRs) and was placed on the biceps and triceps of the upper arm.

As shown in Figure 13, the FSRs were connected in series with reference resistors and provided an adjustable voltage of 0–3.3 V through an 8-bit digital-to-analog converter (DAC) of the ESP32 microprocessor board. During the calibration phase, the supply voltage was optimized to ensure the maximum dynamic range and sensitivity of the measurement results. Subsequently, the force myography (FMG) signals were sampled with a frequency of 100 Hz and sent via Bluetooth to MATLABR2022b software for further processing.

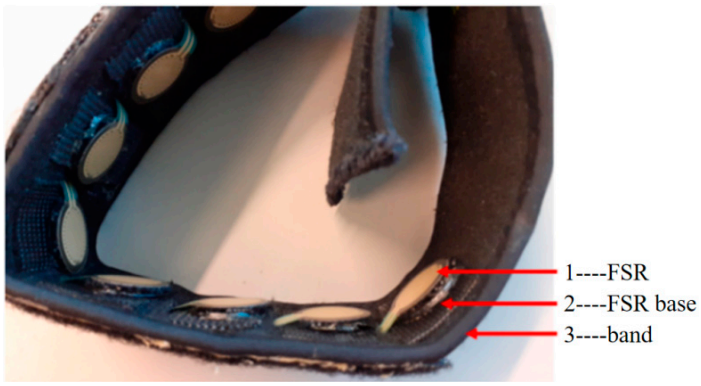


Figure 13. The mounting of the FSR sensor on the sensor band [15].

Stiffness estimation was carried out in this research with FMG. This did not necessitate the connection of a force sensor at the end effector; rather, it only requires an FSR sensor to detect upper arm muscle activity and the joint configuration for payload level estimation. The relevant data of the band are shown in Table 4.

Table 4. BioX AAL-Band 2.0 output channel parameters.

Column Number	Column Name	Measurement
1–8	Force Sensing Resistors	V
9–11	Gravity (x, y, z)	m/s^2
12–14	Angular Velocity (x, y, z)	rad/s
15–17	Linear Acceleration (x, y, z)	m/s^2
18–20	Euler Angle (x, y, z)	deg
21	Time	s

The process of manual handling generally involves lifting, holding, and putting down actions. In this research, the repeated-lifting experiment and the carrying experiment were devised.

The subjects performed the same repeated weightlifting and standing experiments with and without wearing the elbow exoskeleton. Each set of movements was replicated three times, and the muscle stress of the biceps and triceps of the human arm was recorded and compared, respectively, in the two states. To enhance muscle activation, the subjects carried a load of 25 kg to accomplish the handling test. The experimental demonstration process is shown in Figure 14.

In order to obtain more accurate data, the FSR data of eight channels of sensor were collected in this experiment to obtain the average muscle activity for the flexion and extension of biceps and triceps during repeated handling and standing, respectively. The fitting curve for the response of the FSR was established by experiments, and is expressed as Equation (13)

$$V = \alpha \ln(F) - \beta \tag{13}$$

where α and β take values of 0.6904 and 1.3548, respectively, with 11 data points. The estimated stiffness was filtered by a 1 Hz low-pass filter for the control [15].

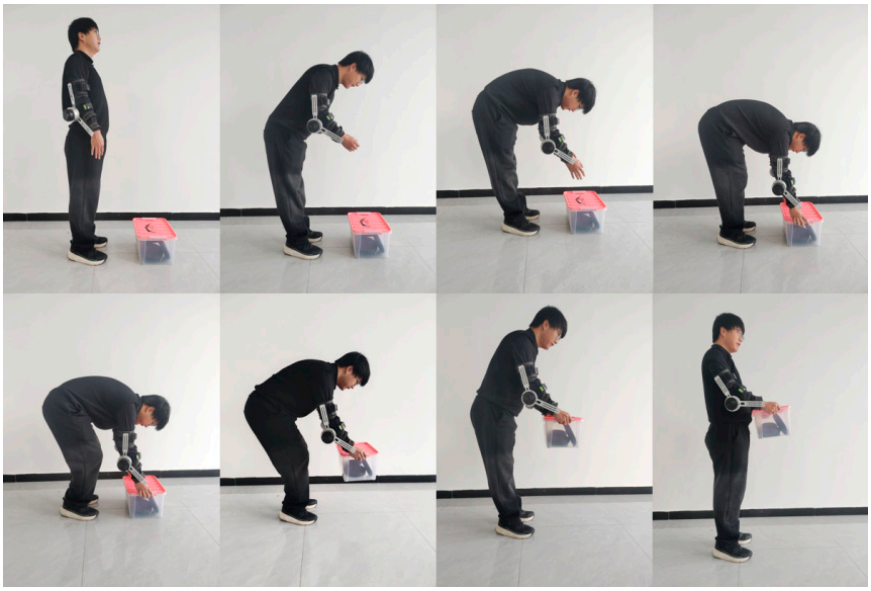
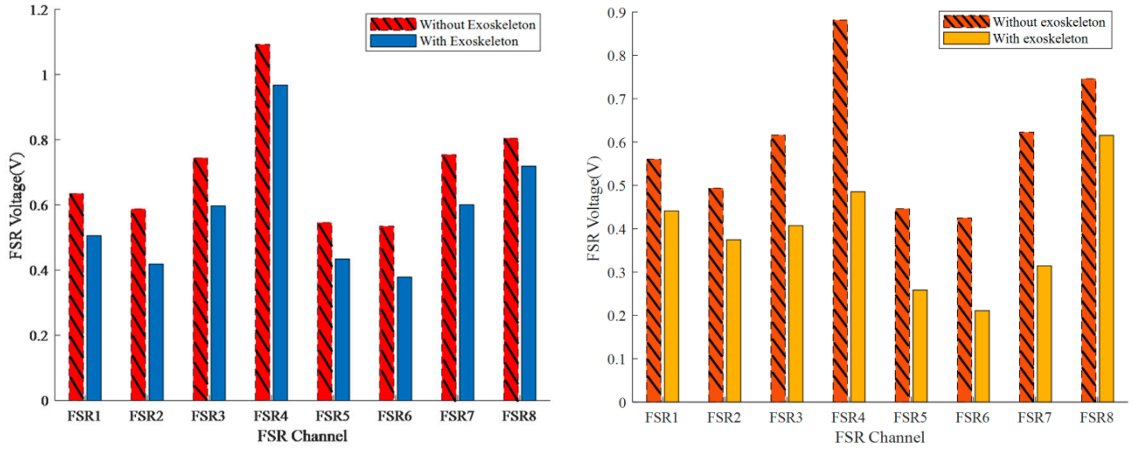


Figure 14. The process of subjects lifting heavy objects.

During the experimental phase, the subjects conducted the continuous transportation experiment. Figure 15 shows the histogram of the FMG mean values of biceps and triceps before and after the extension of the elbow exoskeleton.



(**a**) (**b**)

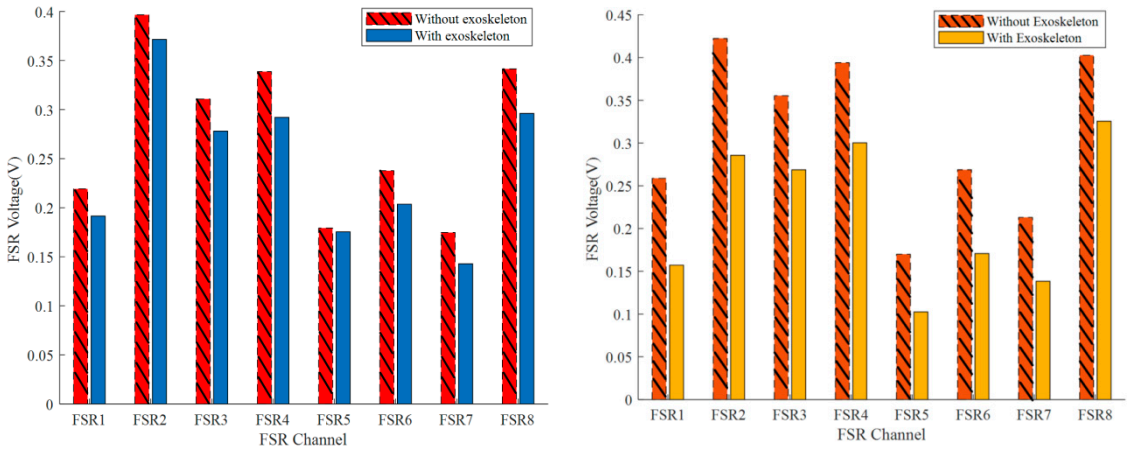
Figure 15. The mean histogram of FSRs for the extension process. (**a**) Histogram of biceps FSR mean during extension. (**b**) Histogram of FSR mean of triceps during extension.

According to Equation (13), the average assisting efficiency of the biceps during the extension is 15.14%, and the average assisting efficiency of triceps muscle in the process of extension is 23.53%.

Figure 16 shows the histogram of FMG mean values of the biceps and triceps before and after the flexion of the elbow exoskeleton.

The average power efficiency of biceps muscle during flexion is 18.34%. The average power efficiency of triceps muscle during flexion is 15.46%.

The mean histogram data show that the elbow exoskeleton can effectively reduce muscle force, which is consistent with the simulation results. During the experiment, the subjects were also able to feel that the muscles were getting a boost from the elbow powered exoskeleton.



(**a**) (**b**)

Figure 16. Mean histogram of FSR for flexion process. (**a**) Histogram of biceps FSR mean during flexion. (**b**) Histogram of triceps FSR mean during flexion.

6. Conclusions

In this research, a wearable and compliant elbow exoskeleton is designed, aiming to eliminate the shortcomings of poor safety performance and complex evaluation methods. We also propose a suitable evaluation process for the effectiveness of the assisted exoskeleton.

The human musculoskeletal model and the associated human–machine system model were developed utilizing the AnyBody Modeling System. This approach facilitated the creation of detailed representations of the human body musculoskeletal structure and its interaction with the designed system. By conducting a comparative analysis of the muscle strength, activation levels, and length curves of the principal arm muscles before and after donning the elbow joint, the power-assisting capabilities of the joint were effectively quantified. Employing the AnyBody performance evaluation method streamlines the experimental workflow, leading to diminished experimental expenditures, a shorter test cycle, and attenuated exposure to risks for the participants.

Based on the simulation outcomes of the AnyBody Modeling System, an experimental platform was used to test muscle activity and assistive performance using the BioX AAL-Band. The findings indicate that the powered wearable compliant elbow joint exoskeleton offers greater power to the human upper limb and demonstrates remarkable practicability and integration in manual material handling.

For future studies, it is important to explore the items of the lightweight structure design of exoskeleton and the improvement of the performance evaluation scheme. Future research could further improve the safety and health analysis of warehouse workers involved in manual material handling tasks and minimize the risk of work-related muscular skeletal disorders (WMSDs).

Author Contributions: Conceptualization, H.Q.; Software, Z.Z.; Validation, J.Z.; Formal analysis, Z.H.; Data curation, L.L.; Writing—original draft, K.L.; Writing—review & editing, R.L. All authors have read and agreed to the published version of the manuscript.

Funding: This work was supported by the Research Project of the Shanxi Scholarship Council of China (2023-135), the Graduate Research Innovation Project of Shanxi Province (2024KY596), and the Key Research and Development Program of Shanxi Province of China (Grant No. 202202150401018).

Data Availability Statement: All data supporting the findings of this study are available within the article. Any additional requests for information can be directed to, and will be fulfilled by, the corresponding author. Source data are provided with this research.

Acknowledgments: We thank the intelligent design and manufacturing team, School of Mechanical Engineering, North University of China, and our participants for their contributions to this work.

Conflicts of Interest: The authors declare that they have no known competing financial interest or personal relationships that could have appeared to influence the work reported in this design.

References

1. Intranuovo, G.; De Maria, L.; Facchini, F.; Giustiniano, A.; Caputi, A.; Birtolo, F.; Vimercati, L. Risk Assessment of Upper Limbs Repetitive Movements in a Fish Industry. *BMC Res. Notes* **2019**, *12*, 354. Available online: https://bmcresnotes.biomedcentral.com/articles/10.1186/s13104-019-4392-z (accessed on 1 January 2025). [CrossRef] [PubMed]
2. Valentim, D.P.; de Oliveira Sato, T.; Comper, M.L.C.; da Silva, A.M.; Boas, C.V.; Padula, R.S. Reliability, Construct Validity and Interpretability of the Brazilian Version of the Rapid Upper Limb Assessment (RULA) and Strain Index (SI). *Braz. J. Phys. Ther.* **2018**, *22*, 198–204. Available online: https://www.sciencedirect.com/science/article/pii/S1413355517306196?via%3Dihub (accessed on 1 January 2025). [CrossRef]
3. Gao, M.; Wang, Z.; Pang, Z.; Sun, J.; Li, J.; Li, S.; Zhang, H. Electrically Driven Lower Limb Exoskeleton Rehabilitation Robot Based on Anthropomorphic Design. *Machines* **2022**, *10*, 266. Available online: https://www.mdpi.com/2075-1702/10/4/266 (accessed on 1 January 2025). [CrossRef]
4. Liu, Z. ULS Robotics: Exoskeleton Robot Helps Industrial Manufacturing Advances in Biomedical Engineering. *Robot. Ind.* **2023**, *1*, 62–65.
5. Sun, B. Maibao Intelligent: Design Exoskeleton Products and Build Evaluation System. *Robot. Ind.* **2022**, *5*, 67–70. Available online: https://kns.cnki.net/kcms2/article/abstract?v=hmawDzFpZzRgHONYVhRCZGEO__SpAMQKNowldU0XF8_y37nyadN-JlNxhzTXnzibTRrqOHIRch-liXjtxnUC4NPQ1eFwpVRoGtw4vPoaNKujt3LcqSHh-CjjFr1YaP4Xcbw2oPI58Hcbp2vJ8rZ613hs6IGTVKScQprepcQJefA0Hob-xDKgtMI07YOXb6Nm&uniplatform=NZKPT&language=CHS (accessed on 1 January 2025).
6. McDevitt, S.; Hernandez, H.; Hicks, J.; Lowell, R.; Bentahaikt, H.; Burch, R.; Ball, J.; Chander, H.; Freeman, C.; Taylor, C.; et al. Wearables for Biomechanical Performance Optimization and Risk Assessment in Industrial and Sports Applications. *Bioengineering* **2022**, *9*, 33. Available online: https://www.mdpi.com/2306-5354/9/1/33 (accessed on 1 January 2025). [CrossRef] [PubMed]
7. Zimmermann, Y.; Song, J.; Deguelle, C.; Läderach, J.; Zhou, L.; Hutter, M.; Riener, R.; Wolf, P. Human-Robot Attachment System for Exoskeletons: Design and Performance Analysis. *IEEE Trans. Robot.* **2023**, *39*, 3087–3105. Available online: https://ieeexplore.ieee.org/document/10120599 (accessed on 1 January 2025). [CrossRef]
8. Islam, M.; Bai, S. Payload Estimation Using Forcemyography Sensors for Control of Upper-Body Exoskeleton in Load Carrying Assistance. *Model. Identif. Control (Online)* **2019**, *40*, 189–198. Available online: https://www.mic-journal.no/PDF/2019/MIC-2019-4-1.pdf (accessed on 1 January 2025). [CrossRef]
9. Du Plessis, T.; Djouani, K.; Oosthuizen, C. A Review of Active Hand Exoskeletons for Rehabilitation and Assistance. *Robotics* **2021**, *10*, 40. Available online: https://www.mdpi.com/2218-6581/10/1/40 (accessed on 1 January 2025). [CrossRef]
10. Gull, M.A.; Bai, S.; Bak, T. A Review on Design of Upper Limb Exoskeletons. *Robotics* **2020**, *9*, 16. Available online: https://www.mdpi.com/2218-6581/9/1/16 (accessed on 1 January 2025). [CrossRef]
11. Islam, M.R.; Brahmi, B.; Ahmed, T.; Assad-Uz-Zaman, M.; Rahman, M.H. Exoskeletons in Upper Limb Rehabilitation: A Review to Find Key Challenges to Improve Functionality. In *Control Theory in Biomedical Engineering*; Academic Press: Cambridge, MA, USA, 2020; pp. 235–265.
12. Tahir, A.; An, Z.; Bai, S.; Shen, M. Robust Payload Recognition Based on Sensor-over-Muscle-Independence Deep Learning for the Control of Exoskeletons. *IEEE Trans. Circuits Syst. II Express Briefs* **2023**, *70*, 3699–3703. Available online: https://ieeexplore.ieee.org/document/10102267 (accessed on 1 January 2025). [CrossRef]
13. Massardi, S.; Rodriguez-Cianca, D.; Pinto-Fernandez, D.; Moreno, J.C.; Lancini, M.; Torricelli, D. Characterization and Evaluation of Human-Exoskeleton Interaction Dynamics: A Review. *Sensors* **2022**, *22*, 3993. Available online: https://www.mdpi.com/1424-8220/22/11/3993 (accessed on 1 January 2025). [CrossRef] [PubMed]
14. Zhang, X.; Shan, G.; Wang, Y.; Wan, B.; Li, H. Wearables, Biomechanical Feedback and Human Motor-Skills' Learning & Optimization. *Appl. Sci.* **2019**, *9*, 226. Available online: https://www.mdpi.com/2076-3417/9/2/226 (accessed on 1 January 2025). [CrossRef]
15. Zhu, Y.; Bai, S.P. Human Compatible Stiffness Modulation of a Novel VSA for Physical Human-Robot Interaction. *IEEE Robot. Autom. Lett.* **2023**, *8*, 3023–3030. Available online: https://ieeexplore.ieee.org/document/10070819 (accessed on 1 January 2025). [CrossRef]

16. Zhi, H. Joint Movement Patterns and Participating Muscle Groups [EB/OL]. (2020-2-23) [2024.12.20]. Available online: https://zhuanlan.zhihu.com/p/72574629 (accessed on 1 January 2025).
17. Matijevich, E.S.; Scott, L.R.; Volgyesi, P.; Derry, K.H.; Zelik, K.E. Combining Wearable Sensor Signals, Machine Learning and Biomechanics to Estimate Tibial Bone Force and Damage During Running. *Hum. Mov. Sci.* **2020**, *74*, 102690. Available online: https://www.sciencedirect.com/science/article/pii/S0167945720305546?via%3Dihub (accessed on 1 January 2025). [CrossRef] [PubMed]
18. *GB/T 10000-2023*; Human Dimensions of Chinese Adults. National Standardization Administration: Beijing, China, 2023. Available online: https://www.renrendoc.com/paper/323366169.html (accessed on 1 January 2025).
19. Bao, G.; Pan, L.; Fang, H.; Wu, X.; Yu, H.; Cai, S.; Yu, B.; Wan, Y. Academic Review and Perspectives on Robotic Exoskeletons. *IEEE Trans. Neural Syst. Rehabil. Eng.* **2019**, *27*, 2294–2304. Available online: https://ieeexplore.ieee.org/document/8853289 (accessed on 1 January 2025). [CrossRef]
20. Nguiadem, C.; Raison, M.; Achiche, S. Motion Planning of Upper-Limb Exoskeleton Robots: A Review. *Appl. Sci.* **2020**, *10*, 7626. Available online: https://www.mdpi.com/2076-3417/10/21/7626 (accessed on 1 January 2025). [CrossRef]
21. Gupta, A.; Singh, A.; Verma, V.; Mondal, A.K.; Gupta, M.K. Developments and Clinical Evaluations of Robotic Exoskeleton Technology for Human Upper-Limb Rehabilitation. *Adv. Robot.* **2020**, *34*, 1023–1040. Available online: https://www.tandfonline.com/doi/full/10.1080/01691864.2020.1749926 (accessed on 1 January 2025). [CrossRef]
22. Vélez-Guerrero, M.A.; Callejas-Cuervo, M.; Mazzoleni, S. Artificial Intelligence-Based Wearable Robotic Exoskeletons for Upper Limb Rehabilitation: A Review. *Sensors* **2021**, *21*, 2146. Available online: https://www.mdpi.com/1424-8220/21/6/2146 (accessed on 1 January 2025). [CrossRef]
23. AbdElmomen, M.; Dengiz, O.; Hoda, S.; Tamre, M. Research on Upper-Body Exoskeletons for Performance Augmentation of Production Workers. In *DAAAM Proceedings*, 1st ed.; Katalinic, B., Ed.; DAAAM International: Vienna, Autria, 2019; Volume 1, pp. 904–913. Available online: https://www.daaam.info/Downloads/Pdfs/proceedings/proceedings_2019/126.pdf (accessed on 1 January 2025).
24. Desbrosses, K. Manual Handling Tasks Performed with an Upper Limbs Exoskeleton at the Workplace. *Ann. Phys. Rehabil. Med.* **2017**, *60*, e101. Available online: https://www.sciencedirect.com/science/article/pii/S1877065717303275?via%3Dihub (accessed on 1 January 2025). [CrossRef]
25. Qu, X.; Qu, C.; Ma, T.; Yin, P.; Zhao, N.; Xia, Y.; Qu, S. Effects of an Industrial Passive Assistive Exoskeleton on Muscle Activity, Oxygen Consumption and Subjective Responses During Lifting Tasks. *PLoS ONE* **2021**, *16*, e0245629. Available online: https://journals.plos.org/plosone/article?id=10.1371/journal.pone.0245629 (accessed on 1 January 2025). [CrossRef] [PubMed]
26. Zhang, H.; Zhao, Y.Y.; Li, J.Y.; Cui, Y.P.; Ynag, G.Q.; Yuan, B. Evaluation of the Performance of a Passive Arm Assisted Exoskeleton. *J. Chongqing Univ. Technol. (Nat. Sci.)* **2023**, *37*, 329–338.
27. Liu, C.; Liang, H.; Ueda, N.; Li, P.; Fujimoto, Y.; Zhu, C. Functional Evaluation of a Force Sensor-Controlled Upper-Limb Power-Assisted Exoskeleton with High Backdrivability. *Sensors* **2020**, *20*, 6379. Available online: https://www.mdpi.com/1424-8220/20/21/6379 (accessed on 1 January 2025). [CrossRef] [PubMed]
28. Kong, Y.K.; Choi, K.H.; Cho, M.U.; Kim, S.Y.; Kim, M.J.; Shim, J.W.; Park, S.S.; Kim, K.R.; Seo, M.T.; Chae, H.S.; et al. Ergonomic Assessment of a Lower-Limb Exoskeleton Through Electromyography and Anybody Modeling System. *Int. J. Environ. Res. Public Health* **2022**, *19*, 8088. Available online: https://www.mdpi.com/1660-4601/19/13/8088 (accessed on 1 January 2025). [CrossRef] [PubMed]
29. Tahir, A.; Bai, S.; Shen, M. A Wearable Multi-Modal Digital Upper Limb Assessment System for Automatic Musculoskeletal Risk Evaluatio. *Sensors* **2023**, *23*, 4863. Available online: https://www.mdpi.com/1424-8220/23/10/4863/xml (accessed on 1 January 2025). [CrossRef] [PubMed]
30. Del Ferraro, S.; Falcone, T.; Ranavolo, A.; Molinaro, V. The Effects of Upper-Body Exoskeletons on Human Metabolic Cost and Thermal Response During Work Tasks-A Systematic Review. *Int. J. Environ. Res. Public Health* **2020**, *17*, 7374. Available online: https://www.mdpi.com/1660-4601/17/20/7374 (accessed on 1 January 2025). [CrossRef]
31. Grazi, L.; Trigili, E.; Proface, G.; Giovacchini, F.; Crea, S.; Vitiello, N. Design and Experimental Evaluation of a Semi-Passive Upper-Limb Exoskeleton for Workers with Motorized Tuning of Assistance. *IEEE Trans. Neural Syst. Rehabil. Eng.* **2020**, *28*, 2276–2285. Available online: https://ieeexplore.ieee.org/document/9159674 (accessed on 1 January 2025). [CrossRef] [PubMed]
32. Weinstock-Zlotnick, G.; Mehta, S.P. A Systematic Review of the Benefits of Occupation-Based Intervention for Patients with Upper Extremity Musculoskeletal Disorders. *J. Hand Ther.* **2019**, *32*, 141–152. Available online: https://www.sciencedirect.com/science/article/pii/S0894113017302910?via%3Dihub (accessed on 1 January 2025). [CrossRef]

Disclaimer/Publisher's Note: The statements, opinions and data contained in all publications are solely those of the individual author(s) and contributor(s) and not of MDPI and/or the editor(s). MDPI and/or the editor(s) disclaim responsibility for any injury to people or property resulting from any ideas, methods, instructions or products referred to in the content.